Research on Engineering Structures & Materials
www.jresm.org
Research Group

Research Article

General analysis of the dissipation of strain energy in circular columns

Victor Rizov[a]

Dept. of Technical Mechanics, University of Architecture, Civil Engineering and Geodesy, Sofia, Bulgaria

Article Info

Article history:

Received 28 Dec 2023
Accepted 16 Apr 2024

Keywords:

Circular Column;
Dissipation of strain energy;
General analysis

Abstract

This theoretical paper is concerned with general analysis of the strain energy dissipation in columns of circular cross-section. The columns are under longitudinal displacements that vary continuously with time. The columns exhibit non-linear viscoelastic behavior that is studied by mechanical models constructed by using non-linear springs and dashpots. Besides, the columns are functionally graded along the radius of the cross-sections. A simple expression for the dissipated strain energy in the columns under consideration is derived. The expression holds for columns having portions with different radius of the cross-section. Also, the expression derived is applicable for columns built-up by concentric layers. Results indicating how the dissipated strain energy is influenced by various factors (distribution of material properties, geometry of the columns and loading) are presented. These results are found by using a non-linear viscoelastic model with one spring and one dashpot. A check-up is performed by determining the dissipated strain energy through subtracting the strain energy in the spring of viscoelastic model from the whole strain energy in the column.

1. Introduction

Since columns are widely used in various load-carrying engineering structures, it is important to study in detail the response of columns to different external loads and influences. Deepening of the knowledge for the column's response is an important condition for improving the safety and reliability of structures.

Dissipation of the strain energy is a momentous factor that has to be considered when studying columns of viscoelastic behavior. For instance, the dissipation of the strain energy has influence on such issues like fracture behavior, structural integrity and expected service-life of engineering constructions and facilities (it should be noted here that when the strain energy dissipation takes place in a structure, the fracture behavior has to be analyzed by using the strain energy cumulated in the structure reduced by the dissipated energy). Therefore, dissipation of the strain energy has to be taken into account in the design and use of structural members (including columns) having viscoelastic behavior. This, on its side, requires analyses of the strain energy dissipation.

The significance of the dissipation of strain energy for engineering structures with viscoelastic behavior is well-grounded in the scientific literature [1]. It should be underlined, however, that the majority of the strain energy analyses have been concerned with linear viscoelastic beam load-bearing structures [1 - 2]. Besides, the analyses usually are focused on particular problems [3 - 7]. The end-plate beam-to-column connection

*Corresponding author: v_rizov_fhe@uacg.bg
[a]orcid.org/0000-0002-0259-3984
DOI: http://dx.doi.org/10.17515/resm2024.134me1228rs

under cyclic loading is evaluated [3]. It is shown that the neutral network model used is capable of characterizing pinching and stiffness degradation of the connection [3]. A

The significance of the dissipation of strain energy for engineering structures with viscoelastic behavior is well-grounded in the scientific literature [1]. It should be underlined, however, that the majority of the strain energy analyses have been concerned with linear viscoelastic beam load-bearing structures [1 - 2]. Besides, the analyses usually are focused on particular problems [3 - 7]. The end-plate beam-to-column connection under cyclic loading is evaluated [3]. It is shown that the neutral network model used is capable of characterizing pinching and stiffness degradation of the connection [3]. A framework that provides an optimal distribution of energy dissipation devices for framed buildings is presented in [4]. It is proved that the proposed framework is superior compared to the conventional machine learning algorithms for obtaining optimum retrofitting scheme for buildings considered [4]. Energy dissipation and damping capacity of reinforced concrete columns under uniaxial and biaxial conditions are investigated in [5]. The energy dissipation is studied in terms of cumulative dissipated energy. The study leads to obtaining of simplified expressions for equivalent viscous damping in columns under biaxial loading conditions [5]. The free vibration behavior of two-directional functionally graded multiple nanobeam systems are analyzed by considering Winkler elastic medium between them in [6]. It is assumed that the material properties very along the length and thickness of the nanobeams. The effects of nonlocal parameter, slenderness ratio, functionally graded power index and boundary conditions are evaluated [6]. A nanobeam with a moving nanoparticle is studied in [7]. A mathematical model for the nanobeam-nanoparticle system is developed. The influence of various factors, including the nonlocal parameter, initial velocity and mass of nanoparticle are studied and discussed [7]. The fact that previous works deal with particular problems indicates that general analysis of the strain energy dissipation needs to be developed.

Therefore, the present paper is concerned with general analysis of the dissipated strain energy in columns exhibiting non-linear viscoelastic behavior. The columns under consideration have circular cross-section. The general analysis is developed assuming that columns are functionally graded along the cross-section radius. This assumption is made in view of the fact that functionally graded materials have become very attractive for a variety of applications in engineering structures and facilities in recent decades [8 - 13]. Due to their excellent properties, the functionally graded materials have begun to replace the widely used up to now homogeneous engineering materials like metals, allows and fiber reinforced composites [14 - 19]. One of the basic advantages of the functionally graded materials is that their properties vary smoothly in a given structural member [20 - 25]. In this way, the stress concentrations are avoided which considerably reduces the probability of loss of stiffness, degradation of strength, shortening of expected service-life and even premature failure of the structure due to appearance and propagations of cracks [26 - 28]. Other widely used structural materials in modern engineering are multilayered systems having a high strength-to-weight and stiffness-to-weight ratio [29]. As known, the multilayered constructions represent systems of adhesively bonded layers made of different materials [30 - 34]. In view of the increased interest towards the multilayered materials and structures, general analysis of the dissipated strain energy is developed in the present paper also for multilayered columns built-up by concentric layers. The layers are functionally graded through thickness and have non-linear viscoelastic behavior.

The general analysis of the strain energy dissipation developed here uses non-linear viscoelastic models constructed by non-linear springs and dashpots. The analysis yielded a relatively simple expression for the dissipated strain energy. This expression holds for functionally graded (and multilayered) circular columns under longitudinal displacements which vary continuously with time. Besides in columns clamped at the bottom, the strain

energy dissipation is analyzed also in columns clamped at the bottom and the top. The results obtained are checked-up by determining the dissipated strain energy by subtracting the strain energy in the spring from the whole strain energy in the columns under consideration. The change of the dissipated strain energy caused by inhomogeneity of the material, the column geometry and the longitudinal displacements magnitude is studied.

2. General Analysis

The general analysis developed here is concerned with strain energy dissipation in the column which static schema is displayed in Fig. 1. The column under consideration has n longitudinal portions.

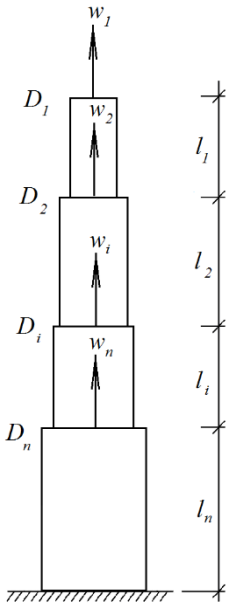

Fig. 1. Column under longitudinal displacements, w_i

The cross-section of the column in each portion is a circle. The radius of the column cross-section in an arbitrary portion is marked by R_i. The length of the column arbitrary portion is marked by l_i (Fig. 1). The bottom of the column is clamped. The column has non-linear viscoelastic mechanical behavior. In an arbitrary column portion, the viscoelastic behavior is described by a stress-strain-time relationship written in the form

$$\sigma_i = f_i(\varepsilon_i, t) \tag{1}$$

$$i = 1, 2, \ldots, n \tag{2}$$

where σ_i is the stress, ε_i is the strain and t is time. It should be underlined that f_i is a non-linear function of the strain. The present strain energy dissipation analysis uses viscoelastic models built-up by non-linear springs and dashpots for describing the column mechanical behavior. Therefore, stress-strain-time relationships (1) are derived by analyzing the stresses and strains in the viscoelastic model components. It should also be

underlined that the mechanical properties involved in the stress-strain-time relationships (1) are smooth functions of the running radius, R, where $0 \le R \le R_i$ due to the fact that in each column portion the material is functionally graded in radial direction.

The column in Fig. 1 is under longitudinal displacements, w_i, which vary smoothly with time (the law controlling this variation is given). The displacements, w_i, are expressed through strains by formula (3), i.e.

$$w_i = \sum_{j=i}^{j=n} \varepsilon_j l_j \tag{3}$$

The strains in the column portions can be easily determined from (3). Then these strains can be applied on the viscoelastic model to determine the stresses. The strain energy dissipation in the column under consideration is modeled by the dashpots in the viscoelastic model. Therefore, the dissipated strain energy, U_{dse}, in the column can be expressed by using formula (4), i.e.

$$U_{dse} = \sum_{i=1}^{i=n} l_i \iint_{(A_i)} \sum_{k=1}^{k=p} u_{0ik} dA \tag{4}$$

where p is the number of dashpots in the viscoelastic model, u_{0ik} is the unit strain energy in the *k*-th dashpot in the *i*-th column portion, A_i is the cross-section area of the column in the *i*-th portion. Formula (5) is applied for determining the unit strain energy.

$$u_{0ik} = \int_0^{\varepsilon_{ik}} \sigma_{ik} d\varepsilon_{ik} \tag{5}$$

$$i = 1, 2, \ldots, n \tag{6}$$

$$k = 1, 2, \ldots, p \tag{7}$$

where σ_{ik} is the stress in the in the *k*-th dashpot of the viscoelastic model in the *i*-th portion of the column. The stress, σ_{ik}, is found by applying relationship (8), i.e.

$$\sigma_{ik} = g_{ik}(\dot{\varepsilon}_{ik}) \tag{8}$$

where $\dot{\varepsilon}_{ik}$ is the first derivative of the strain in the dashpot under consideration with respect to time, g_{ik} is a non-linear function of $\dot{\varepsilon}_{ik}$ (the type of this function depends on the viscoelastic model used).

If the column is built-up by concentric layers (the cross-section of such a column is displayed in Fig. 2) the dissipated energy can be derived by formula (9), i.e.

$$U_{dse} = \sum_{i=1}^{i=n} l_i \sum_{s=1}^{s=m} \iint_{(A_{is})} \sum_{k=1}^{k=p} u_{0isk} dA \tag{9}$$

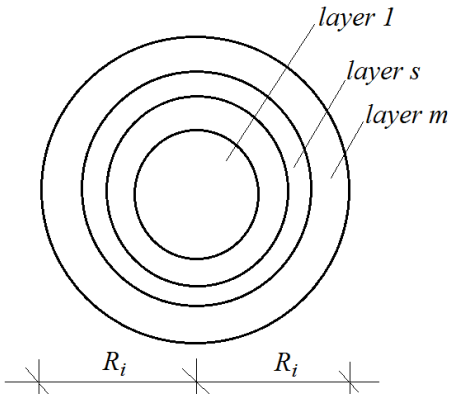

Fig. 2. Cross-section of a column built-up by concentric layers

where m is the number of layers, A_{is} is the cross-section area of the *s*-th layer in the *i*-th portion of the column, u_{0isk} is the unit strain energy in the *k*-th dashpot in the *s*-th layer in the *i*-th column portion. Here formula (10) can be used for deriving u_{0isk}.

$$u_{0isk} = \int_0^{\varepsilon_{isk}} \sigma_{isk} d\varepsilon_{isk} \tag{10}$$

where σ_{isk} and ε_{isk} are the stress and strain, respectively.

General analysis of the dissipated strain energy in columns in which the number of portions is higher than the number of given longitudinal displacements (refer to Fig. 3) can also be developed. For this purpose, additional equations have to be composed for determining the strains in the column portions (this is necessary because the number of equations composed by using (3) is less than the number of unknown strains). These additional equations consider the equilibrium of the axial forces on borders between column portions (for instance, for column in Fig. 3 such equations have to be composed for borders, D_i and D_n). These equations can be written as

$$\iint_{(A_{i-1})} \sigma_{i-1} dA = \iint_{(A_i)} \sigma_i dA \tag{11}$$

where σ_{i-1} and σ_i are the stresses in the column cross-sections over and under border, D_i.

The stresses, σ_{i-1} and σ_i, are found by using the viscoelastic model. If the column is built-up by concentric layers, the additional equations for determining the strains in the column portions have the following form:

$$\sum_{s=1}^{s=m} \iint_{(A_{i-1s})} \sigma_{i-1s} dA = \sum_{s=1}^{s=m} \iint_{(A_{is})} \sigma_{is} dA \tag{12}$$

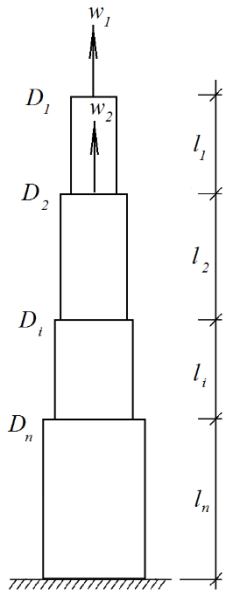

Fig. 3. Column in which the number of portions is higher than the number of longitudinal displacements, w_i

analysis of the dissipated strain energy is developed also for the column that is clamped at the bottom and the top (the column static schema is displayed in Fig. 4). Here again the column is under longitudinal displacements, w_i.

The displacement of the column top is zero. Thus, we write

$$w_{D1} = \sum_{i=1}^{i=n} \varepsilon_i l_i = 0 \tag{13}$$

Also, we can write (Fig. 4)

$$w_i = \sum_{j=i}^{j=n-1} \varepsilon_{j+1} l_{j+1} \tag{14}$$

Where;

$$i = 1, 2, \ldots, n-1 \tag{15}$$

The strains in the column portions can be derived directly from equations (13) and (14). After that the dissipated strain energy can be obtained by using (4). If the column is made of concentric layers, the dissipated strain energy can be found by applying formula (9).

For columns in which the number of portions is higher than the number of the given longitudinal displacements like, for instance, column in Fig. 5, the strains can be derived by using additional equations of equilibrium (11) (or (12) when the column is made by concentric layers). After that formula (4) (or formula (9)) can be used for obtaining of dissipated strain energy.

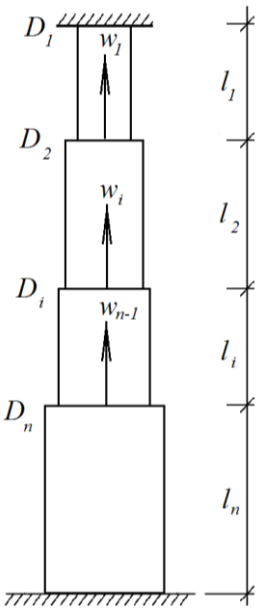

Fig. 4. Column clamped at the bottom and the top

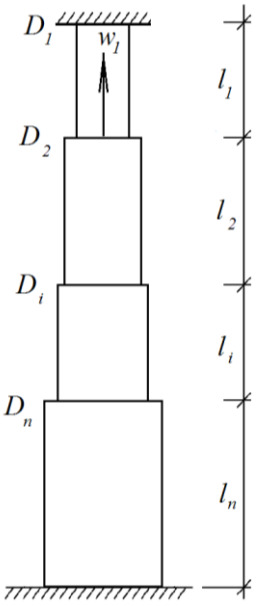

Fig. 5. Column clamped at the bottom and the top in which the number of portions is higher than the number of longitudinal displacements, w_i

3. Practical Application of General Analysis

This section of the paper describes practical applications of the general analysis of the dissipated strain energy. The numerical results presented here are related to the functionally graded viscoelastic column with three portions displayed in Fig. 6.

The column is under longitudinal time-dependent displacements, w_i, where $i = 1, 2, 3$. Formula (16) describes the change of these displacements.

$$w_i = w_{ib} \cos(a_0 + \omega t) \tag{16}$$

where w_{ib}, a_0 and ω are parameters.

The strains, ε_1, ε_2 and ε_3, in the column portions, D_1D_2, D_2D_3 and D_3D_4, are determined from equation (3) with taking into account (16). The result is;

$$\varepsilon_1 = \frac{1}{l_1}(w_{1b} - w_{2b}) \cos(a_0 + \omega t) \tag{17}$$

$$\varepsilon_2 = \frac{1}{l_2}(w_{2b} - w_{3b}) \cos(a_0 + \omega t) \tag{18}$$

$$\varepsilon_3 = \frac{1}{l_3} w_{3b} \cos(a_0 + \omega t) \tag{19}$$

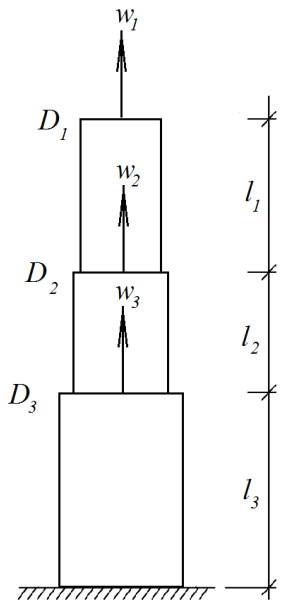

Fig. 6. Column with three portions under three longitudinal displacements, w_1, w_2 and w_3

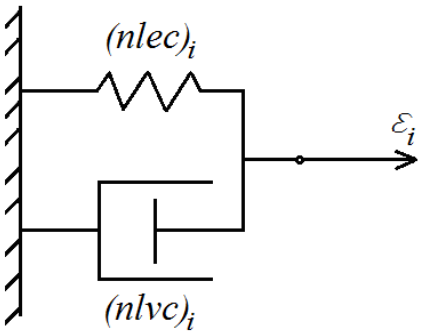

Fig. 7. Non-linear viscoelastic model

The stresses in the column portions are derived by using the non-linear viscoelastic mechanical model displayed in Fig. 7. This model has a non-linear elastic spring, $(nlvc)_i$, and a non-linear dashpot, $(nlec)_i$. The model is under strain, ε_i, whose change with time is presented by formulas (17), (18) and (19) for column portions, D_1D_2, D_2D_3 and D_3D_4, respectively. The choice of a relatively simple non-linear viscoelastic model (Fig. 7) with one spring and one dashpot is motivated by the fact that this model is mainly for illustration of the way for use of the general analysis. When a practical engineering problem is treated, a more complex non-linear viscoelastic model with more springs and dashpots may be applied.

Formula (20) defines the stress-strain relationship of the non-linear elastic spring in the viscoelastic model in Fig. 7 [35].

$$\sigma_{(nlec)i} = Q_i\left[1-\left(1-\frac{\varepsilon_i}{H_i}\right)^{\beta_i}\right] \tag{20}$$

where $\sigma_{(nlec)i}$ is the stress in the spring, Q_i, H_i and β_i are material properties in the *i*-th portion of the column (here $i=1,2,3$). According to [35], Q_i is the ultimate strength, H_i is the strain that corresponds to the ultimate strength, β_i is the ratio of the

initial modulus of elasticity to the secant modulus at the ultimate strength (usually, $\beta_i \geq 1$ [35]).

The constitutive relationship of the non-linear dashpot in the model shown in Fig. 7 is described by formula (21) [35], i.e.

$$\sigma_{(nlvc)i} = L_i\left[1-\left(1-\frac{\dot{\varepsilon}_i}{B_i}\right)^{\delta_i}\right] \tag{21}$$

where $\sigma_{(nlvc)i}$ is the stress in the dashpots, $\dot{\varepsilon}_i$ is the first derivative of the strain with respect to time, L_i, B_i and δ_i are material properties in the *i*-th portion of the column (here again $i=1,2,3$). The stress, σ_i, in the viscoelastic model is determined as (Fig. 7)

$$\sigma_i = \sigma_{(nlec)i} + \sigma_{(nlvc)i} \tag{22}$$

In fact, formula (22) presents the stress-strain-time relationship of the non-linear viscoelastic model. Since the column is functionally graded in radial direction, the material properties, Q_i, H_i, β_i, L_i, B_i and δ_i, which are involved in (20), (21) and (22) vary smoothly along the radius of the column cross-section. This variation is described by the following formulas:

$$Q_i = Q_{0i}e^{\alpha_i\frac{R}{R_i}} \tag{23}$$

$$H_i = H_{0i}e^{\varphi_i\frac{R}{R_i}} \tag{24}$$

$$\beta_i = \beta_{0i}e^{\lambda_i\frac{R}{R_i}} \tag{25}$$

$$L_i = L_{0i}e^{\mu_i\frac{R}{R_i}} \tag{26}$$

$$B_i = B_{0i}e^{\theta_i\frac{R}{R_i}} \tag{27}$$

$$\delta_i = \delta_{0i}e^{\rho_i\frac{R}{R_i}} \tag{28}$$

Where;

$$0 \leq R \leq R_i \tag{29}$$

$$i = 1,2,3 \tag{30}$$

In formulas (23) – (29), Q_{0i}, H_{0i}, β_{0i}, L_{0i}, B_{0i} and δ_{0i} are the values of Q_i, H_i, β_i, L_i, B_i and δ_i in the center of the column cross-section, α_i, φ_i, λ_i, μ_i, θ_i and ρ_i are parameters which control the variation of the material properties.

Formula (22) can be used to calculate the stress in the column portions with taking into account the change of the material properties in the radial direction via formulas (23) – (28).

The dissipated strain energy in the column is determined by applying formula (4) (here $n=3,\ p=1$). The unit strain energy, u_{0ik}, in the dashpot of the viscoelastic model that is involved in (4) is determined by replacing of σ_{ik} with $\sigma_{(nlvc)i}$ in formula (5). The MATLAB is used for integration in (4).

The dissipated strain energy solution for the column in Fig. 6 is checked-up in the following way. First, the axial forces, F_1, F_2 and F_3, in column cross-sections, D_1, D_2 and D_3, are derived by using the following dependences:

$$F_1 = \iint\limits_{(A_1)} \sigma_1 dA \tag{31}$$

$$F_2 = \iint\limits_{(A_2)} \sigma_2 dA - \iint\limits_{(A_1)} \sigma_1 dA \tag{32}$$

$$F_3 = \iint\limits_{(A_3)} \sigma_3 dA - \iint\limits_{(A_2)} \sigma_2 dA \tag{33}$$

where A_1, A_2 and A_3 are the areas of the column cross-section in portions, D_1D_2, D_2D_3 and D_3D_4, respectively (Fig. 6). Substitution of (22) in (31), (32) and (33) yields

$$F_1 = \iint\limits_{(A_1)} \left[\sigma_{(nlec)1} + \sigma_{(nlvc)1} \right] dA \tag{34}$$

$$F_2 = \iint\limits_{(A_2)} \left[\sigma_{(nlec)2} + \sigma_{(nlvc)2} \right] dA - \iint\limits_{(A_1)} \left[\sigma_{(nlec)1} + \sigma_{(nlvc)1} \right] dA \tag{35}$$

$$F_3 = \iint\limits_{(A_3)} \left[\sigma_{(nlec)3} + \sigma_{(nlvc)3} \right] dA - \iint\limits_{(A_2)} \left[\sigma_{(nlec)2} + \sigma_{(nlvc)2} \right] dA \tag{36}$$

Formula (37) is applied to determine the strain energy, U, in the column.

$$U = \int_0^{w_1} F_1 dw_1 + \int_0^{w_2} F_2 dw_2 + \int_0^{w_3} F_3 dw_3 \tag{37}$$

The unit strain energy, u_{0i}, in the non-linear elastic spring of the viscoelastic model in Fig. 7 is found by formula (38), i.e.

$$u_{0i} = \int_0^{\varepsilon_i} \sigma_{(nlec)i} d\varepsilon_i \tag{38}$$

where the stress, $\sigma_{(nlec)i}$, in the spring is determined by using relationship (20). Then u_{0i} is integrated in the three portions of the column (Fig. 6), i.e.

$$U_{nlec} = \sum_{i=1}^{i=3} l_i \iint_{(A_i)} u_{0i} dA \tag{39}$$

Finally, the dissipated strain energy, U_{dse}, in the column is derived by subtracting of U_{nlec} from U.

$$U_{dse} = U - U_{nlec} \tag{40}$$

Actually, formula (40) is based on the fact that the spring in the viscoelastic model in Fig. 7 preserves the strain energy. Therefore, by subtracting of the strain energy in the spring, U_{nlec}, from the whole strain energy, U, we should derive the dissipated strain energy, U_{dse}.

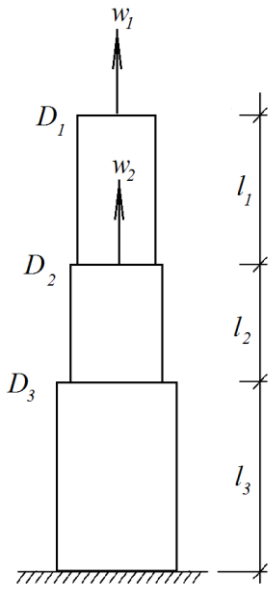

Fig. 8. Column with three portions under two longitudinal displacements, w_1 and w_2

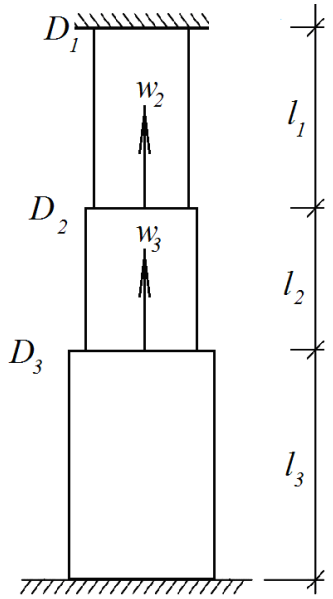

Fig. 9. Column clamped at the bottom and the top and having three portions under two longitudinal displacements, w_2 and w_3

The dissipated strain energy determined by using (40) matches that obtained by applying the general analysis through formula (4) (this is a check-up of the analysis).

The dissipated strain energy is determined also for the column displayed in Fig. 8 (this column is under two longitudinal displacements, w_1 and w_2, which change according formula (16)). From equation (3) we obtain

$$\varepsilon_1 = \frac{1}{l_1}(w_1 - w_2) \tag{41}$$

$$w_2 = \varepsilon_2 l_2 + \varepsilon_3 l_3 \tag{42}$$

where ε_2 and ε_3 are unknown.

One additional equation is written by considering the equilibrium of the axial forces in section, D_3, of the column (Fig. 8), i.e.

$$\iint\limits_{(A_3)} \sigma_3 dA = \iint\limits_{(A_2)} \sigma_2 dA \tag{43}$$

where σ_2 and σ_3 are determined by using (22). Equations (42) and (43) are solved with respect to ε_2 and ε_3. Then the dissipated energy in the column is found by using formula (4) (the result obtained is verified by (40)).

Analysis of the dissipated strain energy in the column clamped at the bottom and the top as displayed in Fig. 9 also is performed. The column is under longitudinal displacements, w_2 and w_3, which change according to formula (16). Equations (13) and (14) are applied for determining the strains, ε_1, ε_2 and ε_3, in the column portions, D_1D_2, D_2D_3 and D_3D_4. The result is

$$\varepsilon_1 = \frac{1}{l_1}(-w_{2b})\cos(a_0 + \omega t) \tag{44}$$

$$\varepsilon_2 = \frac{1}{l_2}(w_{2b} - w_{3b})\cos(a_0 + \omega t) \tag{45}$$

$$\varepsilon_3 = \frac{1}{l_3} w_{3b} \cos(a_0 + \omega t) \tag{46}$$

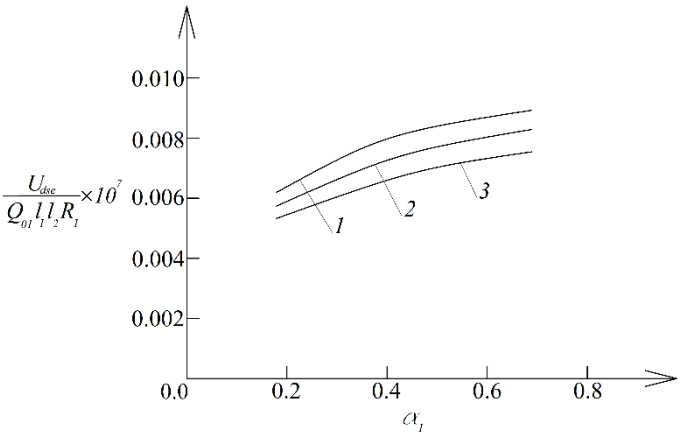

Fig. 10. Change of the normalized dissipated strain energy with increase of α_1 for the column with three portions under three longitudinal displacements, w_1, w_2 and w_3 (curve 1 – at $\varphi_1 = 0.2$, curve 2 – at $\varphi_1 = 0.5$ and curve 3 – at $\varphi_1 = 0.8$)

The viscoelastic model displayed in Fig. 7 is used for treating the column in Fig. 9. The change of material properties along the column cross-section radius is described by formulas (23) – (28). Formula (4) is applied to derive the dissipated strain energy in the column under consideration (Fig. 9). A check-up of the dissipated strain energy solution is carried-out via formula (40).

Further, we assume that the column in Fig. 9 is built-up by concentric layers. The column layers are inhomogeneous through their thickness. Formulas (47) – (52) are used for describing the smooth change of the material properties through thickness of the *s*-th layer in the *i*-th portion of the column.

$$Q_{is} = Q_{0is} e^{\alpha_{is} \frac{R - R_{is-1}}{R_{is} - R_{is-1}}} \tag{47}$$

$$H_{is} = H_{0is} e^{\varphi_{is} \frac{R - R_{is-1}}{(R_{is} - R_{is-1})}} \tag{48}$$

$$\beta_{is} = \beta_{0is} e^{\lambda_{is} \frac{R - R_{is-1}}{R_{is} - R_{is-1}}} \tag{49}$$

$$L_{is} = L_{0is} e^{\mu_{is} \frac{R - R_{is-1}}{R_i - R_{is-1}}} \tag{50}$$

$$B_{is} = B_{0is} e^{\theta_{is} \frac{R - R_{is-1}}{R_{is} - R_{is-1}}} \tag{51}$$

$$\delta_{is} = \delta_{0is} e^{\rho_{is} \frac{R - R_{is-1}}{R_{is} - R_{is-1}}} \tag{52}$$

Where;

$$R_{is-1} \le R \le R_{is} \tag{53}$$

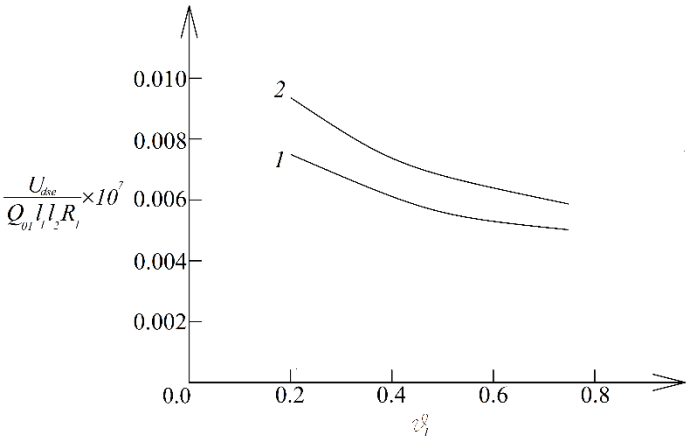

Fig. 11. Change of the normalized dissipated strain energy with increase of θ_1 (curve 1- for the column with three portions under two longitudinal displacements, w_1 and w_2, curve 2 - for the column with three portions under three longitudinal displacements, w_1, w_2 and w_3)

In formulas (47) – (52), Q_{0is}, H_{0is}, β_{0is}, L_{0is}, B_{0is} and δ_{0is} are the values of Q_{is}, H_{is}, β_{is}, L_{is}, B_{is} and δ_{is} at $R = R_{is-1}$ (here R_{is-1} and R_{is} are the radiuses of the internal and external surfaces of the layer, respectively). The dissipated strain energy in the column built-up by concentric layers is determined by applying formula (9). A check-up is performed by using expression (40).

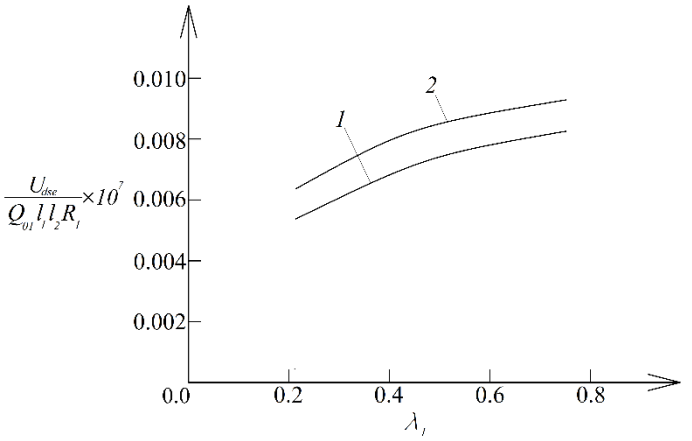

Fig. 12. Change of the normalized dissipated strain energy with increase of λ_1 (curve 1- for the column clamped at the bottom and having three portions under three longitudinal displacements, curve 2 - for the column clamped at the bottom and the top and having three portions under two longitudinal displacements, w_2 and w_3)

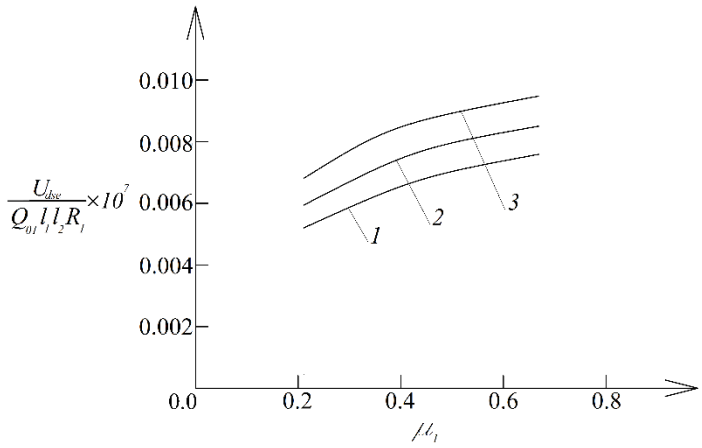

Fig. 13. Change of the normalized dissipated strain energy with increase of μ_1 for column clamped at the bottom and the top and having three portions under two longitudinal displacements, w_2 and w_3 (curve 1 – at $w_{3b} = 0.003$ m, curve 2 – at $w_{3b} = 0.004$ m and curve 3 – at $w_{3b} = 0.005$ m)

The graphs displayed in Fig. 10, Fig. 11, Fig. 12, Fig. 13 and Fig. 14 illustrate how the dissipated strain energy in the non-linear viscoelastic inhomogeneous columns in Fig. 6, Fig. 8 and Fig. 9 changes under the influence of different factors (inhomogeneity of the material, the column geometry, parameters of the longitudinal displacements, etc.).

It is assumed that $l_1 = 2$ m, $l_2 = 3$ m, $l_3 = 4$ m, $R_1 = 0.15$ m, $R_2 = 0.20$ m, $R_3 = 0.25$ m, $Q_{01} = 180000$ kPa, $H_{01} = 0.001$, $\beta_{01} = 1.3$, $L_{01} = 1400$ kPa, $B_{01} = 0.0015$ 1/s, $\delta_{01} = 1.2$ $\omega = 0.0003$ 1/s and $a_0 = 0.1$.

The influence of α_1 and φ_1 on the dissipated strain energy (the latter is presented in normalized (non-dimensional) form) for the column with three portions under three longitudinal displacements (refer to Fig. 6) is displayed in Fig. 10. The graphs in Fig. 10 indicate that the rise of α_1 causes growth of the dissipated strain energy. The rise of φ_1 generates a reduction of the dissipated strain energy (Fig. 10).

Rise of θ_1 causes reduction of the dissipated strain energy as one can observe in Fig. 11. The graphs displayed in Fig. 11 reveal also that the dissipated strain energy in the column with three portions under three longitudinal displacements (refer to Fig. 6) is higher than that in the column with three portions under two longitudinal displacements (refer to Fig. 7).

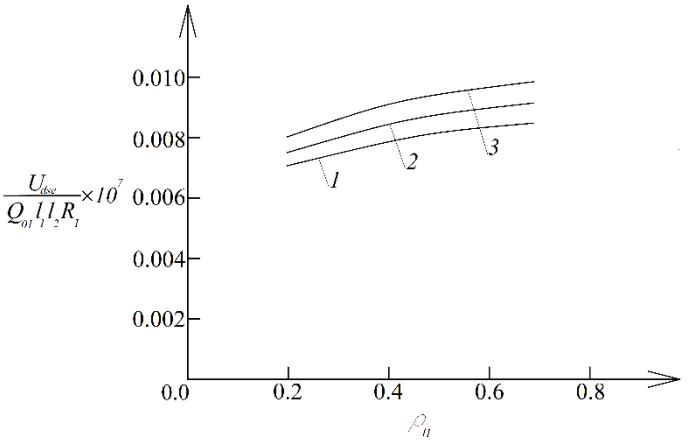

Fig. 14. Change of the normalized dissipated strain energy with increase of ρ_{11} for column clamped at the bottom and the top and having three portions under two longitudinal displacements, w_2 and w_3 (curve 1 – at $l_3/l_1=1.5$, curve 2 – at $l_3/l_1=2.0$ and curve 3 – at $l_3/l_1=2.5$)

The effect of λ_1 is studied for both columns displayed in Fig. 6 and Fig. 9. The corresponding graphs are displayed in Fig. 12. It can be seen that rise of λ_1 causes smooth growth of the dissipated strain energy (Fig. 12). It can also be seen in Fig. 12 that the dissipated strain energy in the column clamped at the bottom and the top (refer to Fig. 9) is higher than that in the column clamped at the bottom end only (refer to Fig.6).

One can observe in Fig. 13 how the dissipated strain energy changes with rise of μ_1 in the column clamped at the bottom and the top (refer to Fig. 9) at three values of w_{3b}. Graphs in Fig. 3 indicate growth of the dissipated strain energy with rise of μ_1 and w_{3b}.

How the dissipated strain energy varies with increase of ρ_{11} in the column clamped at the bottom and the top and built-up by concentric layers (the number of layers is 3, 5 and 7 in column portions, D_1D_2, D_2D_3 and D_3D_4, respectively) can be seen in Fig. 14. The graphs indicate rise of the dissipated strain energy with increase of ρ_{11} at each of the considered l_3/l_1 ratios (Fig. 14).

4. Conclusions

General analysis of the dissipation of the strain energy in columns under continuously varying with time longitudinal displacements is developed. The first step in the analysis is to determine the strains in the column. Then the strains are used to derive stresses. The analysis yields a simple expression for the dissipated strain energy in columns of circular cross-section. The columns are functionally graded in radial direction. Besides, the columns under consideration have non-linear viscoelastic behavior that is analyzed by viscoelastic mechanical models which are structured by using non-linear springs and dashpots. Actually, this is the basic assumption in the present study. This assumption

imposes an important limitation in sense that the approach developed here is applicable only when models with spring and dashpots are used (the dissipated energy is derived from the strain energy in the dashpots). The columns have an arbitrary number of portions with different radius of the cross-section. The general analysis is applicable also for determining of the dissipated strain energy in non-linear viscoelastic columns built-up by concentric layers. Each layer may have different material properties. Besides, the layers may be functionally graded through thickness. The expression obtained is used for determining the dissipated strain energy in a column clamped at the bottom. A column clamped at the bottom and the top also is studied. Since the columns are functionally graded along the radius of the cross-section, the material properties which are involved in the expression for the dissipated strain energy change continuously in radial direction. A check-up of the results obtained is performed by determining the dissipated strain energy by subtracting the strain energy in the spring from the whole strain energy cumulated in the column. It is found that increase of the value of α_1 generates growth of the dissipated strain energy. Growth of the dissipated strain energy is observed also when λ_1, μ_1 and ρ_{11} rise. An opposite behavior, i.e. reduction of the dissipated strain energy is observed when φ_1 and θ_1 rise. The increase of l_3 / l_1 ratio induces rise of the dissipated strain energy (this finding indicates that the dissipated strain energy in longer column is higher). The dissipated strain energy rises also when w_{3b} has higher values. It can be summarized that the main novelty of this paper is in the fact that general analysis of the dissipated energy in non-linear viscoelastic columns is presented. One of the practical implications of the derived expressions and the results is in fracture mechanics. For example, when fracture is analyzed in terms of the strain energy release rate, the latter has to be derived from the strain energy reduced by the dissipated energy that can be determined by applying the expressions obtained in the present paper.

References

[1] Dowling N. Mechanical Behavior of Materials, Pearson, 2007.

[2] Rizov V. Analysis of temperature change effect on dissipation of energy in functionally graded beams. The Eurasia Proceedings of Science, Technology, Engineering & Mathematics (EPSTEM), 2023; 23: 406-412. https://doi.org/10.55549/epstem.1371771

[3] Abdollahzadeh G, Hashemi SM, Tavakoli H et al. Determination of Hysteretic Behavior of Steel End-Plate Beam-to-Column Connection with Mechanical and Neural Network Modeling. Arab J Sci Eng, 2014; 39: 7661-7671. https://doi.org/10.1007/s13369-014-1348-4

[4] Noureldin M, Ali A, Nasab MSE, Kim J. Optimum distribution of seismic energy dissipation devices using neural network and fuzzy inference system. Comput Aided Civ Inf, 2021; 36:1306-1321. https://doi.org/10.1111/mice.12673

[5] Hugo Rodrigues, Humberto Varum, António Arêde, Aníbal Costa. A comparative analysis of energy dissipation and equivalent viscous damping of RC columns subjected to uniaxial and biaxial loading. Engineering Structures, 2012; 35: 149-164. https://doi.org/10.1016/j.engstruct.2011.11.014

[6] Ahmadi I, Davarpanah M, Sladek J et al. A size-dependent meshless model for free vibration analysis of 2D-functionally graded multiple nanobeam system. J Braz. Soc. Mech. Sci. Eng., 2024; 46: 11. https://doi.org/10.1007/s40430-023-04580-5

[7] Isa Ahmadi, Mohammad Naeim Moradi and Mahdi Davar Panah. Dynamic response analysis of nanoparticle-nanobeam impact using nonlocal theory and meshless method. Structural Engineering and Mechanics, 2024; 89: 135-153.

[8] Kieback B, Neubrand A, Riedel H. Processing techniques for functionally graded materials. Materials Science and Engineering: A, 2003; 362: 81-106. https://doi.org/10.1016/S0921-5093(03)00578-1
[9] Chen Y, Lin X. Elastic analysis for thick cylinders and spherical pressure vessels made of functionally graded materials. Computational Materials Science, 2008; 44: 581-581. https://doi.org/10.1016/j.commatsci.2008.04.018
[10] Dias CMR, Savastano JrH, John V.M. Exploring the potential of functionally graded materials concept for the development of fiber cement. Construction and Building Materials, 2010; 24: 140-146. https://doi.org/10.1016/j.conbuildmat.2008.01.017
[11] Tokovyy Y, Ma CC. Three-Dimensional Elastic Analysis of Transversely-Isotropic Composites. Journal of Mechanics, 2017; 33: 821-830. https://doi.org/10.1017/jmech.2017.91
[12] Tokovyy Y, Ma CC. Elastic Analysis of Inhomogeneous Solids: History and Development in Brief. Journal of Mechanics, 2019; 18: 1-14. https://doi.org/10.1017/jmech.2018.57
[13] Tokovyy Y. Solutions of Axisymmetric Problems of Elasticity and Thermoelasticity for an Inhomogeneous Space and a Half Space. Journal of Mathenatical Science, 2019; 240: 86-97. https://doi.org/10.1007/s10958-019-04337-3
[14] Gandra J, Miranda R, Vilaça P, Velhinho A, Teixeira J.P. Functionally graded materials produced by friction stir processing. Journal of Materials Processing Technology, 2011; 211: 1659-1668. https://doi.org/10.1016/j.jmatprotec.2011.04.016
[15] Zhang Y, Ming-jie Sun, Zhang D. Designing functionally graded materials with superior load-bearing properties. Acta Biomaterialia, 2012; 8: 1101-1108. https://doi.org/10.1016/j.actbio.2011.11.033
[16] Tejaswini N, Babu R, Ram S. Functionally graded material: an overview. Int J Adv Eng Sci Technol, 2013;4: 183-188.
[17] Minoo Naebe, Kamyar Shirvanimoghaddam. Functionally graded materials: A review of fabrication and properties. Applied materials today, 2016; 5; 223-245. https://doi.org/10.1016/j.apmt.2016.10.001
[18] Toudehdehghan J., Lim W., Foo1 K.E., Ma'arof M.I.N., Mathews J. A brief review of functionally graded materials. MATEC Web of Conferences, 2017; 131: 03010. https://doi.org/10.1051/matecconf/201713103010
[19] Nikbakht S, Kamarian S, Shakeri M. A review on optimization of composite structures Part II: Functionally graded materials. Composite Structures, 2019; 214: 83-102. https://doi.org/10.1016/j.compstruct.2019.01.105
[20] El-Galy IM, Saleh BI, Ahmed M.H. Functionally graded materials classifications and development trends from industrial point of view. SN Appl. Sci., 2019; 1: 1378-1389. https://doi.org/10.1007/s42452-019-1413-4
[21] Ekrem Tufekci, Ugurcan Eroglu, Serhan Aydin Aya (2016) Exact solution for in-plane static problems of circular beams made of functionally graded materials. Mechanics Based Design of Structures and Machines, 2016; 44: 476-494. https://doi.org/10.1080/15397734.2015.1121398
[22] Hilal Koc & Ekrem Tufekci (2023) A novel approach of bending behavior of carbon nanotubes by combining the effects of higher-order boundary conditions and coupling through doublet mechanics. Mechanics of Advanced Materials and Structures. https://doi.org/10.1080/15376494.2023.2263767
[23] Tufekci E, Aya SA, Oldac O. A unified formulation for static behavior of nonlocal curved beams. Structural Engineering and Mechanics, 2016; 59: 475-502. https://doi.org/10.12989/sem.2016.59.3.475
[24] Mahamood RM, Akinlabi ET. Functionally Graded Materials, Springer, 2017. https://doi.org/10.1007/978-3-319-53756-6

[25] Shrikantha Rao S, Gangadharan KV. Functionally graded composite materials: an overview, Procedia Materials Science, 2014; 5: 1291-1299. https://doi.org/10.1016/j.mspro.2014.07.442
[26] Saiyathibrahim A, Subramaniyan R, Dhanapl P. Centrefugally cast functionally graded materials - review, In: International Conference on Systems, Science, Control, Communications, Engineering and Technology, 2016; 68-73.
[27] Miyamoto Y, Kaysser WA, Rabin BH, Kawasaki A, Ford RG. Functionally Graded Materials: Design, Processing and Applications, Kluwer Academic Publishers, Dordrecht/London/Boston, 1999. https://doi.org/10.1007/978-1-4615-5301-4
[28] Butcher RJ, Roussea, CE, Tippur HV. A functionally graded particulate composite: Measurements and Failure Analysis, Acta. Mater., 1999; 47: 259-268. https://doi.org/10.1016/S1359-6454(98)00305-X
[29] Rzhanitsyn AR. Built-up Bars and Plates, Stroyiizdat, 1986.
[30] Dolgov NA. Effect of the elastic modulus of a coating on the serviceability of the substrate-coating system. Strength of Materials, 2002; 37: 422-431. https://doi.org/10.1007/s11223-005-0053-7
[31] Dolgov NA. Determination of Stresses in a Two-Layer Coating, Strength of Materials, 2005; 37: 422-431. https://doi.org/10.1007/s11223-005-0053-7
[32] Dolgov NA. Analytical Methods to Determine the Stress State in the Substrate-Coating System Under Mechanical Loads, Strength of Materials, 2016; 48: 658-667. https://doi.org/10.1007/s11223-016-9809-5
[33] Finot M, Suresh S. Small and large deformation of thick and thin-film multilayers: effect of layer geometry and compositonal gradients. J Mech Phys Solids, 1996: 44; 683-721. https://doi.org/10.1016/0022-5096(96)84548-0
[34] Kim JS, Paik KW, Oh SH. The Multilayer-Modified Stoney's Formula for Laminated Polymer Composites on a Silicon Substrate. J. Appl. Phys., 1999; 86: 5474-5479. https://doi.org/10.1063/1.371548
[35] Lukash P. Fundamentals of non-linear structural mechanics, Stroiizdat, 1978.